

Section 1

PROGRESS IN LASER FUSION

1.A Recent Gas-Filled Implosion Experiments on OMEGA

Several experimental campaigns have been successfully carried out on OMEGA since the 24-beam UV system was brought on line in 1985. Initial experiments were devoted to thin-walled glass-shell targets filled with low pressures of DT, in order to obtain high yields and check out the system as a whole. Neutron yields of up to 3×10^{11} were obtained, more than a factor of ten higher than had been obtained on the system in the IR. However, the targets performed in a semi-ablative mode, with the glass shell decompressing from radiation preheat as the implosion proceeded, and the use of a low fuel mass resulted in high fuel temperatures but low densities. Although optimum for neutron production at 1–3 kJ, this mode of implosion does not scale adequately with laser energy. Subsequent series of experiments have therefore been devoted to ablative implosions, with thicker glass walls, which yield higher compressed densities. It is the ablative mode of implosion that scales to ignition and high gain, but, unfortunately, it is the ablative mode that is more susceptible to irradiation nonuniformities and hydrodynamic instabilities. Our experiments have therefore concentrated on two key issues: (1) attempting to achieve nearly one-dimensional implosions; and (2) obtaining and diagnosing high densities.

A series of cryogenic experiments has addressed the second of these issues, and resulted in the first direct measurement of high laser-fusion fuel areal density. Compressed DT fuel densities in the range 20–40 g cm⁻³, i.e., 100–200 times the density of liquid DT, were

achieved, the highest yet attained in direct-drive inertial fusion experiments. These experiments were reported in Refs. 1-3.

In order to investigate the first issue, the conditions required for the attainment of nearly one-dimensional implosions, we have used primarily gas-filled spherical targets that implode ablatively. Indeed, much of the experimental effort on OMEGA from 1986 to 1989 has been devoted to the implosion of these targets, with the primary emphasis being placed on determining the sensitivity of target performance to irradiation nonuniformity. In this article we report results from an extensive series of recent experiments using these targets. We have found that: (a) the yield, expressed as a fraction of the ideal, calculated, one-dimensional yield, decreases with increasing convergence ratio (initial radius divided by final fuel radius); and (b) as a result of the recent improvements in laser uniformity obtained on the OMEGA system, the observed yield has increased to become closer to the one-dimensional calculated yield.

Experimental Conditions

Typical targets for these experiments have been glass shells of wall thickness $\Delta R_0 \sim 3\text{--}6 \mu\text{m}$ and radius $R_0 \sim 100\text{--}150 \mu\text{m}$, filled with D_2 or DT to pressures of 10-100 atm, and irradiated with up to 1.5 kJ of 351-nm light in pulses of $\sim 700\text{-ps}$ duration. These targets are calculated to have relatively modest in-flight aspect ratios ($R/\Delta R \lesssim 30$), and to stagnate with a wide range of convergence ratios depending on the gas pressure and shell thickness. Compressed fuel densities of up to ~ 50 times liquid density have been demonstrated for these targets. While higher densities have been obtained for cryogenic targets, gas-filled targets are better suited for studying the effects of irradiation nonuniformity because of the greater complexity of the cryogenic system; in particular, possible initial nonuniformities associated with cryogenic fuel layers are avoided.

A comprehensive set of plasma, x-ray, and nuclear diagnostics has been deployed to characterize these implosions and to permit comparison with hydrodynamic code calculations. Emphasis has been placed on those diagnostics that provide information on compressed fuel conditions.⁴ The principal diagnostics are neutron dosimetry, neutron time-of-flight spectrometry,⁵ shell-areal-density measurement by neutron activation,⁶ fuel-areal-density measurement by knock-on ion spectrometry,⁷ x-ray microscopy,⁸ time-resolved x-ray photography,⁹ and, in later experiments, multiframe x-ray photography.¹⁰⁻¹² In addition, some estimates of the fuel areal density were obtained from measurements of the secondary-reaction products of D_2 -filled targets.¹³⁻¹⁵

The fraction of laser energy absorbed by the target and the fraction converted into x rays have generally been found to be in good agreement with the predictions of the one-dimensional hydrodynamic code *LILAC*, assuming modest ($f = 0.06$) thermal flux inhibition.¹⁶ The absorption fraction is dependent on the thickness of the shell, as well as the incident intensity (which varied between 5×10^{14} and $1.5 \times 10^{15} \text{ W/cm}^2$ in these experiments). As an example, the

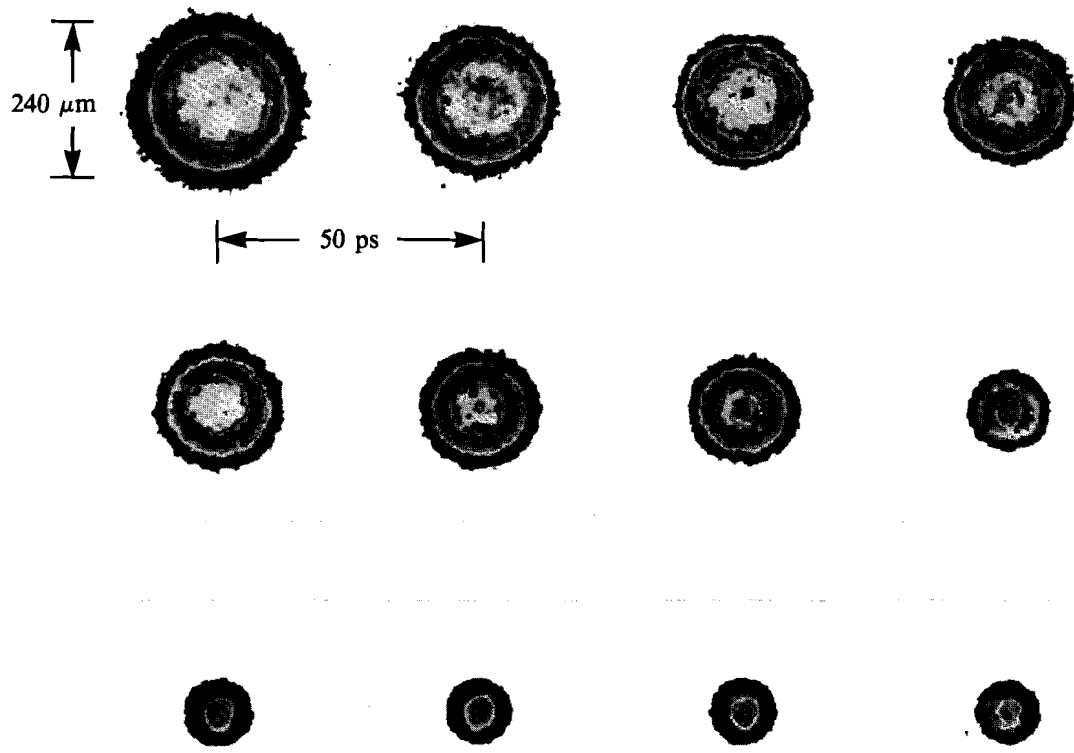
absorption fraction for 4- μm -thick glass shells varied from $\sim 65\%$ at $5 \times 10^{14} \text{ W/cm}^2$ to $\sim 55\%$ at $1.5 \times 10^{15} \text{ W/cm}^2$, in agreement with one-dimensional *LILAC* simulations to within $\pm 5\%$ throughout this intensity range. Similar agreement between theory and experiment was also found for absorption and x-ray-conversion fractions, over a broad intensity range, in early 24-beam UV experiments carried out on spherical solid-glass targets.¹⁷

X-Ray-Framing Camera Images

A greatly improved visualization of the implosion process has been made possible by the recent development of an x-ray-framing camera. This is a pinhole camera outfitted with a fast gating system developed at LLNL¹⁰⁻¹² that provides up to sixteen frames with a temporal resolution of 90 ps. It is filtered to respond to x-ray energies above 1.5 keV; for glass shells the images are dominated by silicon *K*-shell line emission. The spatial resolution of the pinhole camera is 12 μm , although the actual resolution of an individual frame is inevitably degraded somewhat by the motion of the target during the 90-ps time window. An example of an implosion diagnosed with this system is shown in Fig. 40.1, for a 5.1- μm -thick glass shell of initial diameter 250 μm filled with 25 atm of D_2 . The target has already partly imploded by the time of the first frame; the bright region of maximum emission corresponds approximately to the outer surface of the glass shell where the density and electron temperature are both high. Formation of the compressed core can clearly be seen in the later frames, and good implosion symmetry is evident. Implosion asymmetries are detected far more readily in such framing-camera images than in time-integrated x-ray pinhole photographs.¹¹

Streak Camera Images

The implosion history of the same target was also measured using x-ray streak photography (see Fig. 40.2), with the slit of a streak camera placed across the center of an x-ray pinhole image giving 15- μm spatial resolution. Nonlinearity in the streak speed is measured and corrected for by using a series of 100-ps, 351-nm pulses from the DEL laser passed through an etalon. In order to highlight the structure of the image, which is dominated by core emission at the time of peak implosion, two cycles are used on a nonlinear intensity scale; thus, the x-ray intensity at zero radius ($r = 0$) steadily increases with time up to 0.4 ns, and steadily decreases with radius at 0.4 ns. The solid lines superposed upon the experimental image give the *LILAC* predictions for the radius of maximum emission at each time. (Near stagnation, increasing emission from the fuel core causes this radius to jump to the center of the core.) The relative offset between the calculated and experimental time axes has been adjusted to provide the best match, since the absolute experimental timing is not known. Very close agreement is seen throughout the implosion phase. After stagnation, however, some disagreement can be perceived: for example, the core is slightly displaced to positive radius, and the disassembly trajectory for $r > 0$ agrees better with the code than that for $r < 0$. This data is in accord with the general understanding that the effects of irradiation nonuniformity are manifest primarily at the time of stagnation.



E5174

Fig. 40.1
X-ray images of an imploding D_2 -filled target taken with a multiframe gated intensifier system coupled to an x-ray pinhole camera.

The conditions at stagnation become hard to resolve when the predicted core size becomes comparable to the resolution of the pinhole camera. With the proposed OMEGA Upgrade, greatly improved diagnosis of the crucial stagnation phase will be possible: the targets will scale to about three times their present diameter, and the ratio of the initial diameter to the smallest resolvable feature in the compressed core will increase by approximately the same factor. In addition, to improve diagnosis of the compressed core, we plan to implement an x-ray microscope with sub- $5\text{-}\mu\text{m}$ system resolution in front of the framing and streak cameras.

Target Performance

Since a wide variety of targets has been shot in these experiments, we have found it convenient to measure the target performance in relation to the ideal, calculated, one-dimensional yield. The yield, normalized in this way, is plotted as a function of calculated

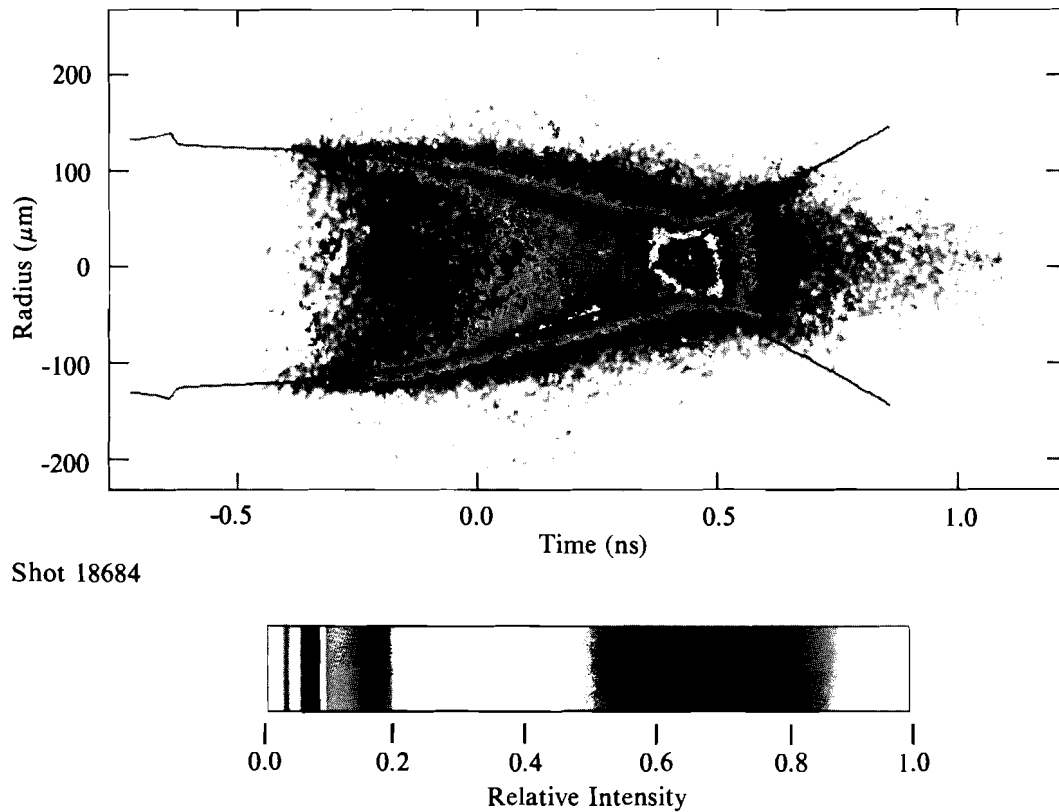


Fig. 40.2 Implosion history of a D_2 -filled target recorded by an x-ray imaging streak camera. The trajectory of maximum x-ray emission calculated using *LILAC* is superposed (solid line).

convergence ratio in Fig. 40.3, for targets with shell thickness in the range $2.5\text{--}3.5\ \mu\text{m}$. The open circles correspond to data taken before the implementation of the uniformity improvements on OMEGA (including phase conversion,¹⁸ SSD,¹⁹⁻²¹ and beam energy and power balance²²). The solid circles correspond to 1989 shots on the improved OMEGA laser, mostly with SSD. In both sets of data it is seen that targets that stagnate with fairly large core sizes ($\geq 30\ \mu\text{m}$, or convergence ratio ≤ 10) produce near to one-dimensional yields; these targets maintain good symmetry throughout the implosion. However, as the expected convergence ratio of the target increases, the measured yield is degraded.

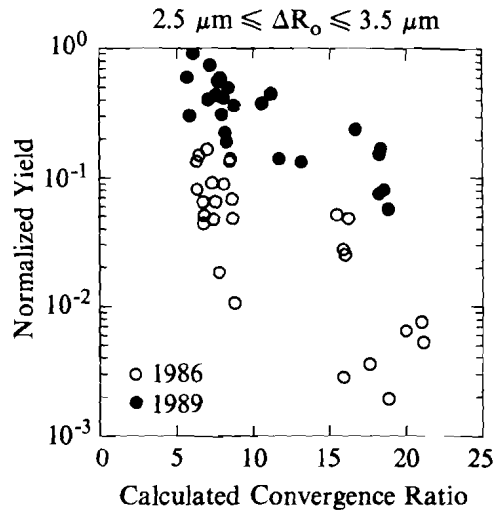
The most notable feature of Fig. 40.3 is the dramatic improvement seen between the early experiments of 1986 and the more recent experiments of this year. Qualitatively similar results have been obtained for other ranges of wall thickness. Much of the scatter is due to the range of target parameters and laser conditions represented in the figure. In order to examine more quantitatively the effect of SSD, with factors such as beam quality, beam energy, and power balance held constant, two series of shots were taken in which the only parameter changed was the laser bandwidth. The D_2 -filled glass shells

used had a diameter of 250 μm and a shell thickness of 5 μm , and were coated with a thin layer of aluminum (see below); the two series corresponded to fill pressures of 25 atm and 10 atm, which have calculated convergence ratios of 17 and 23, respectively. The normalized yield is plotted as a function of bandwidth in Fig. 40.4. Laser conditions on all shots were comparable, except for one shot (the open box) where an amplifier in the driver line misfired, reducing the total system energy but not affecting the uniformity. Substantial improvements are clearly seen using SSD, by factors of 7 and 4, respectively, for the 25-atm and 10-atm targets.

The apparent lack of further improvement for bandwidths greater than 1 \AA is interesting, since theory would predict steady improvement: clearly, the larger the frequency difference between interfering DPP elements, the faster should be the smoothing. One plausible explanation of these observations is suggested by the elliptical beam that is formed from the (hexagonal) DPP elements (see Fig. 37.34 of Ref. 21). At higher bandwidths, more energy is deflected towards the edge of the target and the symmetry of irradiation may be compromised. This problem should be straightforward to resolve using stretched hexagonal phase-plate elements; however, quantification of the improvements obtainable with SSD under a variety of conditions, and optimization of the SSD parameters, merits further experimentation.

The experiments on gas-filled targets have included measurements of secondary-reaction products from D_2 -filled microballoons, i.e., secondary protons from $\text{D}-^3\text{He}$ reactions and secondary neutrons from $\text{D}-\text{T}$ reactions, where the ^3He and the tritons are generated from the two primary $\text{D}-\text{D}$ reactions. These products are detected with activation counters, liquid scintillation counters, a plastic scintillator coupled to a microchannel photomultiplier, and filtered CR-39 track detectors. Ratios of the reaction products can yield information about the fuel temperature and ρR ; they also indicate that mix between the shell and the fuel is occurring in these experiments. The error bars associated with these measurements are often large on account of the poor statistics associated with the low reaction-product yields. With the greater energies anticipated for the OMEGA Upgrade, these measurements will provide significantly improved diagnostics of the core conditions.

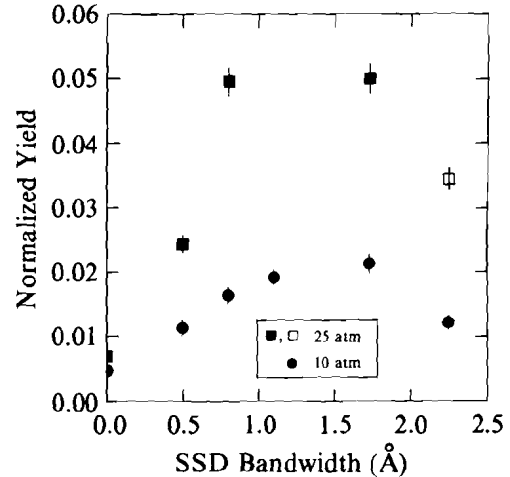
A number of experiments have also been carried out with thick layers of low- Z polymer (parlylene) coated over a 3- μm -thick glass shell. The addition of the polymer should reduce the level of radiative preheat of the fuel, and, depending on the ablator thickness, produce a colder (lower isentrope) implosion leading to higher fuel densities. However, from time-resolved x-ray line spectroscopy of special signature-layer targets,^{23,24} we have obtained evidence of anomalous early lightup of inner regions of the shell. This phenomenon is most probably associated with intense hot spots in the beam distribution [although an alternative explanation in terms of the Rayleigh-Taylor instability has recently been proposed (see Article 1.B on p. 173 in this issue)]. Even with SSD, which causes oscillation of the on-target



TC2620

Fig. 40.3

Yield normalized to one-dimensional *LILAC* predictions as a function of calculated convergence ratio, for DT and D₂-filled glass microballoons of various wall thicknesses (2.5–3.5 μm) and fill pressures. Open circles: data taken in 1986 before the implementation of improvements to the irradiation uniformity. Solid circles: data taken in 1989.



Shots 18512-29

TC2618

Fig. 40.4

Yield normalized to one-dimensional *LILAC* predictions as a function of the full-width IR bandwidth out of the SSD phase modulator, for 5-μm-thick glass targets of diameter 250 μm containing 10 atm (circles) and 25 atm (squares) of D₂. For all points at each fill pressure, other laser and target parameters were held constant.

hot spots associated with the DPP diffraction pattern (which would be static in the absence of SSD), this effect may not be suppressed, probably because the current modulation frequency of 2.5 GHz is insufficient. However, better target performance has often been obtained (even for glass shells) with the addition of a very thin barrier layer of aluminum to the outside of the target. This phenomenon is not properly understood.

Summary

To summarize these gas-filled implosion experiments, the target hydrodynamics agrees very well with *LILAC* predictions for most of the implosion, but discrepancies are found in the last phases of the implosion around the time of stagnation. This is presumably as a result of irradiation nonuniformities. The core conditions at stagnation are difficult to diagnose, especially for high-convergence-ratio targets, because the core sizes are close to the instrumental resolution limit and secondary-reaction yields are too low at laser energies of ~1 kJ. Improvements in laser uniformity, including SSD, have led to greatly improved target performance for convergence ratios up to 25.

ACKNOWLEDGMENT

This work was supported by the U.S. Department of Energy Office of Inertial Fusion under agreement No. DE-FC03-85DP40200 and by the Laser Fusion Feasibility Project at the Laboratory for Laser Energetics, which has the following sponsors: Empire State Electric Energy Research Corporation, New York State Energy Research and Development Authority, Ontario Hydro, and the University of Rochester. Such support does not imply endorsement of the content by any of the above parties.

REFERENCES

1. R. L. McCrory, J. M. Soures, C. P. Verdon, F. J. Marshall, S. A. Letzring, S. Skupsky, T. J. Kessler, R. L. Kremens, J. P. Knauer, H. Kim, J. Delettrez, R. L. Keck, and D. K. Bradley, *Nature* **335**, 225 (1988).
2. LLE Review **35**, 97 (1988).
3. F. J. Marshall, S. A. Letzring, C. P. Verdon, S. Skupsky, R. L. Keck, J. P. Knauer, R. L. Kremens, D. K. Bradley, T. Kessler, J. Delettrez, H. Kim, J. M. Soures, and R. L. McCrory, to be published in *Phys. Rev. A* (1989).
4. M. C. Richardson, R. L. Keck, S. A. Letzring, R. L. McCrory, P. W. McKenty, D. M. Roback, J. M. Soures, C. P. Verdon, S. M. Lane, and S. G. Prussin, *Rev. Sci. Instrum.* **57**, 1737 (1986).
5. S. A. Letzring, G. Pien, L. M. Goldman, M. C. Richardson, and J. M. Soures, *Rev. Am. Phys. Soc.* **30**, 1481 (1985).
6. E. M. Campbell, W. M. Ploeger, P. H. Lee, and S. M. Lane, *Appl. Phys. Lett.* **36**, 965 (1980).
7. S. Kacenjar, L. M. Goldman, A. Entenberg, and S. Skupsky, *J. Appl. Phys.* **56**, 2027 (1984).
8. M. C. Richardson, G. G. Gregory, R. L. Keck, S. A. Letzring, R. S. Marjoribanks, F. J. Marshall, G. Pien, J. S. Wark, B. Yaakobi, P. D. Goldstone, A. Hauer, G. S. Stradling, F. Ameduri, B. L. Henke, and P. A. Jaanimagi, in *Laser Interaction and Related Plasma Phenomena*, Vol. 7, edited by H. Hora and G. H. Miley (Plenum Press, New York, 1986), p. 179.
9. G. G. Gregory, S. A. Letzring, M. C. Richardson, and C. D. Kilkka, in *High Speed Photography, Videography, and Photonics III*, Vol. 569, (SPIE, Bellingham, WA, 1985), p. 141; G. G. Gregory, P. A. Jaanimagi, P. W. McKenty, S. A. Letzring, and M. C. Richardson, *SPIE* **832**, 383 (1987).
10. J. D. Kilkenny *et al.*, *Rev. Sci. Instrum.* **59**, 1793 (1988).
11. D. K. Bradley, J. Delettrez, P. Jaanimagi, F. J. Marshall, C. P. Verdon, J. D. Kilkenny, and P. E. Bell, in *High Speed Photography, Videography and Photonics VI*, Vol. 981 (SPIE, Bellingham, WA, 1989), p. 176.
12. P. E. Bell, J. D. Kilkenny, G. Power, R. Bonner, and D. K. Bradley, in *Ultra High Speed, High Speed Photography and Videography and Photonics VII* (1989), to be published.